Stability of virtual network topology control for overlay routing services

Yuki Koizumi,[1,*] Takashi Miyamura,[2] Shin'ichi Arakawa,[1] Eiji Oki,[2]
Kohei Shiomoto,[2] and Masayuki Murata[1]

[1] *Graduate School of Information Science and Technology, Osaka University, 1-5 Yamadaoka, Suita, Osaka 565-0871, Japan*

[2] *NTT Network Service Systems Laboratories, 3-9-11 Midori-cho, Musashino, Tokyo 180-8585, Japan*

[*] *Corresponding author: ykoizumi@ist.osaka-u.ac.jp*

Overlay networks achieve new functionality and enhance network performance by enabling control of routing at the application layer. However, this approach results in degradations of underlying networks due to the selfish behavior of overlay networks. In this paper, we discuss the stability of virtual network topology (VNT) control under overlay networks that perform dynamic routing updates. We find that the dynamics of routing on overlay networks cause a high fluctuation in the traffic demand matrix, which leads to significant VNT control instability. To overcome this instability, we introduce three extensions, *hysteresis*, *two-state utilization hysteresis*, and *filtering*, to VNT control. Simulation results show that the hysteresis mechanism improves network stability, but cannot always improve network performance. We therefore extend the hysteresis mechanism and show that it improves both network stability and performance. However, this extension requires a lot of time for the VNT to converge to a stable state. To achieve fast convergence, we use a filtering method for VNT control. Through simulations, we prove that our methods achieve stability against overlay routing without loss of adaptability for changes in traffic demand.

OCIS codes: 060.4250, 060.4258.

1. Introduction

A Wavelength Division Multiplexing (WDM) network offers a flexible network infrastructure by utilizing wavelength-routing capability. In such a wavelength-routed WDM network, a set of optical transport channels, called lightpaths, are established between nodes via optical cross-connects (OXCs). Much research has been devoted to methods of carrying IP traffic, which is the majority of Internet traffic, over a wavelength-routed WDM network [1–7]. One approach for accommodating

IP traffic on a wavelength-routed WDM network is to configure a *virtual network topology* (VNT), which consists of lightpaths and IP routers. To achieve effective transport of traffic, *VNT control*, which configures the VNT on the basis of traffic demand, has been investigated in many papers [8,9].

Overlay networks have recently received much attention as a way to achieve new functionality and enhance network performance over IP networks. One of the key technologies in overlay networks lies in overlay routing [10,11]. The fundamental idea of overlay routing is to construct a logical network above the IP network and to allow routing to be controlled on that logical topology. In the literature, a virtual network topology provided by a set of lightpaths is sometimes called "logical topology". In this paper, we use the term "logical topology" in the context of an overlay's logical topology, and we use the term "VNT" for virtual network topology provided by lightpaths. Each overlay node measures the status, such as throughput and delay, of the underlying network, and determines the appropriate route to destination nodes on the overlay network to improve performance and resilience. The resilient overlay network (RON) architecture was proposed in [10]. The RON provides fast detection and recovery from network failures and performance degradation using the existing Internet infrastructure as the underlay network. Another architecture is Detour [11]. It is revealed in [11] that a large percentage of flows can locate better alternative routes by relaying among overlay nodes, which improves the performance of those flows.

As the amount of traffic generated by overlay networks increases, the dynamics of overlay routing have significant impact on VNT control. One typical type of impact is the selfish behavior of overlay routing, as discussed in [12]. Since overlay nodes independently select their route in a selfish manner to optimize their own performance, system-wide performance may not be optimized [13]. Another impact on VNT control is the high variance in the traffic demand induced by overlay routing. Since origin-destination pairs in overlay networks traverse several source-destination pairs in IP networks, the traffic demand of the IP networks strongly depends on the overlay routing. When the VNT is reconfigured in response to changes in the traffic demand due to overlay routing, the network status measured at the overlay network may change. This leads to re-adaptation of the overlay network via overlay routing, which in turn changes in the traffic demand for VNT control. In this way, coexistence of overlay routing and VNT control leads to a high variance in the traffic demand, as we will demonstrate in Section 2.

The interaction between overlay routing and packet layer traffic engineering (TE) has been studied in many papers. In the packet layer TE, the routing of IP traffic is controlled to satisfy its quality requirements. In [12], it is revealed that interaction between overlay routing and packet layer TE causes degradation in the performance of packet layer TE. They argue that the main reason for this degradation is a conflict between two different routing objectives performed at each layer. The impact of selfish routing in intra-domain networks was also investigated in [14]. According to [14], selfish routing can achieve almost optimal performance if an underlay network performs static routing. However, if packet layer TE is used, the performance of the packet layer TE is degraded due to the interaction between overlay routing and packet layer TE. However, these papers show that the performance of packet layer TE is degraded in terms of maximum link utilization, network cost, and average latency. Since VNT is configured on the basis of traffic demand, fluctuations in traffic

demand induced by overlay routing are much more severe for VNT control.

In this paper, we discuss a network architecture in which an overlay network performs dynamic routing in accordance with its own policy above a VNT. We first show that overlay routing highly degrades the performance of VNT control. Then we focus on the VNT control instability caused by the interaction between overlay routing and VNT control. Simulation results show that the instability appears in link utilization, traffic demand, and VNTs due to VNT control. To overcome this instability and achieve a stable VNT control method against overlay routing services, we propose three extensions for VNT control. First, to improve the stability of VNT control, we introduce *hysteresis*, which absorbs traffic demand fluctuations. We show that simple hysteresis applications can improve stability, but cannot always improve performance. We extend the hysteresis application, *two-state utilization hysteresis*, and show that this extension can improve both the stability and performance of VNT control. However, this extension requires a lot of time for the VNT control to become stable. Thus, we achieve faster convergence by using a *filtering* method. Finally, we show that our methods can adapt to changes in the traffic demand, and we therefore achieve stable and feasible VNT control against overlay routing.

The rest of this paper is organized as follows. In Section 2, we discuss performance degradations of the underlay network and show that the coexistence of overlay routing and VNT control results in significant underlay network instability. We introduce hysteresis to overcome this instability in Section 3 and show that simple hysteresis applications cannot improve performance. Because of this, we extended the hysteresis application, as described in Section 4. Although the extended application can improve both stability and performance, it takes a long time for the VNT control to become stable. Therefore, we introduce a filtering method and achieve faster convergence, as described in Section 5. Finally, we conclude this paper in Section 6.

2. Instability of Network State

In this section, we investigate the influence of overlay routing on dynamically configured VNT. Through simulation experiments, we show that the presence of overlay routing services increases the maximum link utilization of the VNT. We also show that the coexistence of overlay routing and VNT control leads to VNT instability.

2.A. Network Model

In our view, a network consists of three layers: an optical layer, a packet layer, and an overlay layer, as shown in Fig. 1. On the optical layer, the WDM network consists of OXCs and optical fibers. The VNT control configures lightpaths between IP routers via OXCs on the WDM network and, these lightpaths and the IP routers form a VNT. On the packet layer, packets are forwarded along the routes that are determined by IP routing on this VNT. On the overlay layer, overlay nodes built on the packet layer form an overlay network. In this network, two types of traffic are carried over the VNT: traffic from overlay networks and traffic from non-overlay networks, which are illustrated as solid and dashed arrows in Fig. 1, respectively. We refer to "*overlay traffic*" as the traffic in the overlay network and to "*non-overlay traffic*" as the traffic in the non-overlay network. We also use

the term "*underlay traffic*" for all traffic on the VNT, which contains both overlay and non-overlay traffic.

Figure 1 shows an example of a network. In this figure, the VNT that has six IP routers and nine links is configured on the WDM network that has six OXCs and six fibers. On the VNT, three overlay nodes, 1, 5, and 6, which are built on IP routers 1, 5, and 6, respectively, form an overlay network, and these nodes are interconnected with overlay links. Solid arrows show overlay traffic from overlay nodes 1 to 6, and dashed arrows show non-overlay traffic from IP routers 1 to 6. Routes for overlay traffic on an overlay network are determined by overlay routing. The overlay traffic in this figure is forwarded from overlay nodes 1 to 6 by relaying through overlay node 5. First, the overlay traffic is sent to overlay node 5. Overlay links are IP tunnels over the VNT in the sense that the traffic on the overlay links is forwarded on the VNT and their routes are determined by IP routing. Thus, the traffic on the overlay link between overlay nodes 1 and 5 is forwarded along the route determined by IP routing, that is, from IP routers 1 to 5 through router 2 on the VNT. The overlay traffic is then forwarded from overlay nodes 5 to 6 in the same way. The non-overlay traffic is forwarded from IP routers 1 to 6 through router 3, which is also controlled by IP routing. The underlay traffic is transported on the WDM network in a similar way as that of the overlay traffic in the sense that lightpaths are transport tunnels over the WDM network and their routes are decided by VNT control. Thus, the underlay traffic from IP routers 1 to 3 is transported from OXCs 1 to 3 via OXC 2. In this paper, we discuss an interaction between the overlay routing and VNT control through the IP layer. Before we introduce this interaction, we describe overlay routing and VNT control more precisely.

2.B. Overlay Routing

Several routing policies for overlay networks, such as overlay selfish routing and overlay optimal routing, have been proposed and evaluated in many papers [14–16]. We use overlay selfish routing, in which each overlay node selects the route that has the largest available bandwidth. This selection is done in a selfish manner aiming at maximizing the throughput experienced by the overlay nodes. The available bandwidth a_l on link l is calculated as $a_l = c_l - x_l$, where c_l is the capacity of link l, and that along route r is represented by $a(r) = \min_{l \in r}(a_l)$. The overlay network selects the route r that satisfies $a(r) = \max_{i \in R} a(i)$, where R denotes the set of all possible routes.

Several papers have proposed means for improving the performance of the overlay network by relaxing the selfishness or greediness of overlay routing [15, 16]. Moreover, selfish routing of which metric of the route selection is the available bandwidth is one of the greediest overlay routing services, as reported in [16]. In this paper, since our objective is to obtain a robust VNT control method against selfish and greedy overlay networks, we use the overlay network that selects the route with the most available bandwidth and do not assume that it uses the previously mentioned cooperative approaches.

2.C. VNT Control

The VNT is configured on the basis of its performance objective by the VNT control method. Several performance objectives for selecting VNTs have been investigated in [17–19]. These investigations have aimed at minimizing the average weighted number of hops, minimizing the maximum link utilization, minimizing the average delay, and maximizing single hop traffic. Many VNT control algorithms for achieving those performance objectives have been investigated [9,20–22]. Since the link utilization directly affects the available bandwidth, which the overlay network seeks to optimize, we use algorithms for minimizing the maximum link utilization to investigate the interaction between overlay routing and VNT control. For minimizing the maximum link utilization, we investigated the MLDA (Minimum delay Logical topology Design Algorithm) [9] and the e-MLDA (extended MLDA) [20]. The MLDA aims to minimize average delay as its performance objective by solving the RWA problem, but the main objective for configuring VNTs is to minimize the maximum link utilization. The e-MLDA is proposed as an extension of the MLDA to ensure accommodation of the traffic demand. The e-MLDA also tries to decrease the maximum link utilization in the network by taking into account the minimum hop IP routing. All these algorithms configure VNTs on the basis of traffic demand to optimize their performance objectives. Note that VNT control cannot distinguish between the traffic demand caused by the overlay and non-overlay traffic. The VNT control uses only combined traffic demand, that is, the traffic demand caused by the underlay traffic. Hereafter, we refer to the traffic demand caused by overlay traffic, non-overlay traffic, and underlay traffic as "overlay traffic demand", "non-overlay traffic demand", and "underlay traffic demand", respectively.

2.D. Interaction Between Overlay Routing and VNT Control

A model for evaluating an interaction between overlay routing and packet layer TE was introduced in [12]. Their model consists of an overlay layer and a packet layer. In this paper, we introduce an optical layer to that model and evaluate the interaction between overlay routing and VNT control through the packet layer. Figure 2 shows our model. When the overlay network switches routes, the overlay traffic demand changes. In response to this traffic change, VNT control reconfigures its VNT. This reconfiguration updates the available bandwidth. The overlay network again switches to a new route that is superior to the previous one to improve the throughput of the overlay traffic. In our simulation experiments, each layer performs the above-mentioned actions and updates their status alternately. More specifically, overlay routing makes its decisions at odd rounds, and VNT control reconfigures its topology at even rounds. We use an OSPF routing protocol for the routing in the packet layer. Since the main purpose of our current research is to investigate the interaction between overlay routing and VNT control, shortest hop paths are used for forwarding traffic on the packet layer.

2.E. Simulation Model

We evaluated the interaction described above with the maximum link utilization, which is the total amount of traffic on a link divided by its capacity since the main objective of the MLDA and

e-MLDA is to minimize the maximum link utilization. We noted that links are overloaded if the utilization exceeds 1, and in this case, no bandwidth is available at these links. We set the capacity of a lightpath to 1, that is, the link capacity was equivalent to the number of lightpaths, and all traffic used in our evaluation was normalized by the capacity of a lightpath.

In our simulation, the overlay network constructs a fully-connected topology in the same way as the environments described in [10,14]. We also placed overlay nodes on all IP routers. Each overlay node independently searched for the route with the largest available bandwidth in a selfish manner. We assigned a proportion of the underlay traffic demand, D, as overlay traffic demand, D_o, and the rest as non-overlay traffic demand, D_n, that is, the traffic demand of the overlay traffic was $D_o = \alpha \cdot D$, and that of the non-overlay traffic was $D_n = (1 - \alpha) \cdot D$.

We used the European Optical Network (EON) topology with 19 nodes and 39 bidirectional links (Fig. 3) for the physical topology. To simplify the interaction model, we did not take into account the wavelength continuity constraint in these experiments, that is, we assumed that all nodes have full wavelength converters on all input and output ports and each node has 8 ports for each direction (i.e., 8 input ports and 8 output ports). We used a randomly-generated traffic demand in the following evaluations.

2.F. Degradation of Underlay Network Performance

The main objective of this section is to discuss the influence that overlay routing has on VNT control. For the purposes of comparison, we used fiber topologies, on which lightpaths are statically configured on a single fiber, i.e., the VNT is equivalent to the physical topology, and the configured topology is fixed.

We show the maximum link utilization in Fig. 4. In this figure, the horizontal axis shows the total amount of traffic demand, and the vertical axis shows the maximum link utilization. We observed that the maximum link utilization increases as the proportion of the overlay traffic increases in the case of all the VNT control algorithms. With a small amount of overlay traffic ($\alpha = 0.1$), the maximum link utilization of the MLDA and e-MLDA with overlay traffic is twice as large as the result without overlay traffic, and a slight degradation is observed in the case of the fiber topology. Although the utilization of the fiber topology gets larger as α increases, the utilization of the MLDA and e-MLDA increases much more severely compared with the result of the fiber topology. This degradation is caused by two factors. One is due to the interaction between overlay nodes, and the other is due to the interaction between overlay routing and VNT control. We refer to the interaction between overlay routing and VNT control as the "*vertical interaction*" and the interaction between overlay nodes as the "*horizontal interaction*". Note that only the horizontal interaction appears in the fiber topology since no VNT reconfiguration occurs. In the case of the MLDA and e-MLDA, both the vertical interaction and horizontal interaction degrade the maximum link utilization since a VNT is reconfigured in response to the dynamics of overlay routing. By comparing the results of the MLDA or e-MLDA with the results of the fiber topology, we can see that the vertical interaction has more effect than the horizontal interaction on the degradation of the maximum link utilization.

2.G. Instability due to Coexistence of Two Routing Mechanisms

In the previous section, we showed that the vertical interaction between overlay routing and VNT control degraded the maximum link utilization. In this section, we show that the coexistence of both overlay routing and VNT control leads to VNT control instability.

Figure 5 shows that the maximum link utilization depends on the rounds at which VNT control or overlay routing takes their actions. As we described above, for the all VNT control method, the maximum link utilization increases if the amount of the overlay traffic is larger than 0.1. Therefore, we set α to 0.2, as shown in this figure, and looked for causes of the degradation mentioned above. When a VNT is dynamically controlled, (i.e., the MLDA or e-MLDA is applied), the fluctuation of the maximum link utilization is larger and the cycle of the fluctuation is irregular. That is, the network becomes unstable due to the vertical interaction.

Figure 6 shows the fluctuation of the traffic volume on each link. The error bars show the maximum and minimum values of the traffic volume in the evaluation, and a point in the bar indicates the average value during the simulation. The horizontal axis represents the link index that is specified uniquely by the source-destination pair. For the all VNTs, the traffic volume of almost all links fluctuates. This result indicates that the horizontal interaction fluctuates the traffic volume on each link. However, the vertical influence is significant in the traffic demands for source-destination pairs on the VNT. Figure 7 shows the maximum, minimum, and average traffic demand for each node pair. We also observed that the traffic demand fluctuates drastically when the VNT is dynamically controlled via the MLDA or e-MLDA. If overlay routing and VNT control coexist on the same network, the network state becomes unstable and its performance is drastically degraded. The main reason for this instability is that the VNT control algorithms generate VNTs on the basis of the current traffic demand. As shown in Fig. 7, if there is selfish overlay routing in the network, the traffic demand drastically changes. Since the traffic demand is the most important input parameter for designing VNTs, traffic demand fluctuation leads to a significant VNT control instability.

3. Improving Stability of Network State

3.A. Applying Hysteresis

In this section, we apply *hysteresis* to VNT control in order to overcome the problem of vertical interaction. Hysteresis is the property of systems that do not immediately react to forces applied to them. This property is often used to avoid routing fluctuation [10, 16, 23].

As discussed in the previous section, the traffic demand heavily fluctuates in the case that overlay routing and VNT control coexist. Because the traffic demand is the input parameter of the VNT control algorithms, applying hysteresis to the traffic demand in order to suppress the influence imposed by overlay routing is one possible application. We refer to this application as "*demand hysteresis*". Another application is *utilization hysteresis*, in which the hysteresis property is used for the maximum link utilization. In the case of utilization hysteresis, the current VNT is kept if the improvement in the link utilization of the new VNT is less than a particular hysteresis threshold. We

expect this leads to a decrease in the number of VNT reconfigurations. We describe each application in more detail in the following sections.

3.A.1. Demand Hysteresis

Demand hysteresis works as follows. Let $D(t) = \{d_p(t)\}$ denote the traffic demand for node pair p at the round t and $D(t-2)$ denote the previously observed traffic demand at round $t-2$. Note that the overlay network updates its routes at round $t-1$. We first temporarily calculate a VNT $C^h(t)$ using the current traffic demand $D(t)$. The VNT $C^h(t)$ is represented by a set of $c_p^h(t)$, where $c_p^h(t)$ is the capacity between node pair p at round t. We then compare the traffic demand $d_p(t)$ with $d_p(t-2)$ for each node pair. If the current traffic demand $d_p(t)$ decreases below the ratio of H_l or increases above the ratio of H_u, we use $c_p^h(t)$ as the new capacity for node pair p. Otherwise, $c_p(t-2)$ is kept. More precisely, $c_p(t)$, where $C(t) = \{c_p(t)\}$ is the VNT that is actually used as the IP layer topology, is updated by the following equations.

$$c_p(t) = \begin{cases} c_p^h(t) & \text{if } d_p(t) > (1+H_u) \cdot d_p(t) \\ c_p^h(t) & \text{if } d_p(t) < (1-H_l) \cdot d_p(t) \\ c_p(t-2) & \text{otherwise} \end{cases}$$

Demand hysteresis is aimed at stabilizing VNT control by absorbing the fluctuation of the traffic demand and reduces unnecessary topology changes. That is, VNT control, to which demand hysteresis is applied, reacts slowly against the heavy fluctuation of the traffic demand.

3.A.2. Utilization Hysteresis

Utilization hysteresis works as follows. Similar to demand hysteresis, we first temporarily calculate the VNT, $C^h(t)$, using the current traffic demand $D(t)$. We then calculate the expected link utilization $U^h(t)$ using $D(t)$ and $C^h(t)$. We next compare the maximum link utilization $\max(U^h(t))$ with $\max(U(t-1))$, where $U(t-1)$ is the link utilization after the overlay network updates its route. If the improvement in the maximum link utilization is larger than the ratio of H, we use $C^h(t)$ as the new VNT. Utilization hysteresis is formulated as follows.

$$C(t) = \begin{cases} C^h(t) & \text{if } \max(U^h(t)) < (1-H) \cdot \max(U(t-1)) \\ C(t-2) & \text{otherwise} \end{cases} .$$

Utilization hysteresis stabilizes VNT control by keeping the current VNT if there is little benefit of changing to the new VNT.

3.B. Performance Evaluation

We evaluated demand hysteresis and utilization hysteresis via computer simulations. We used the same simulation model as presented in Section 2, but in this section, the MLDA is selected as the VNT control algorithm. In obtaining the following figures, the hysteresis mechanisms are not applied during the first 20 rounds to disregard the transient phase. Figures 8 and 9 show the fluctuation of the maximum link utilization when utilization hysteresis and demand hysteresis are

applied. The vertical axis shows the maximum link utilization, and the horizontal axis shows the rounds. Looking at these figures, we observe that the maximum utilization with utilization hysteresis is stable compared to that without hysteresis. However, in contrast to utilization hysteresis, the maximum utilization still fluctuates for demand hysteresis. The main purpose of demand hysteresis is to decrease the number of changed lightpaths by absorbing the fluctuation of the traffic demand caused by overlay routing. However, decreasing the number of changed lightpaths cannot lead to an improvement in the stability of the maximum link utilization. To explain this more clearly, we evaluated two hysteresis applications, and we compared the number of changed lightpaths to investigate the efficiency of demand hysteresis. The results of our evaluation are shown in Figs. 10 and 11. We define the number of changed lightpaths at round t as $\sum |c_e(t) - c_e(t-2)|$. The number of changed lightpaths is decreased by more than 50% in the case that demand hysteresis is applied. However, demand hysteresis cannot make the number of changed lightpaths zero since traffic demand still fluctuates due to the selfish behavior of overlay routing. In the case of utilization hysteresis, the number of changed lightpaths is always zero if VNT control maintains the current VNT. These results show that the changes in the VNT lead to the fluctuation of the maximum link utilization, even if those changes are small.

More detailed observations of these figures show that the performance does not strongly depend on the decision of the hysteresis threshold H in the case that utilization hysteresis is applied. If a large hysteresis threshold H is used, the VNT control does not immediately react against the changes in the network environments. This means that a large H leads to a worse performance since the VNT configured for the previously observed traffic demand is kept. However, the results shown in Fig. 8 are different from expected results. We changed the ratio of overlay traffic α from 0.2 to 0.3 in Figs. 12 and 13. In Fig. 12, the maximum link utilization of $H = 0.0$ is the lowest, while the utilization of $H = 0.0$ in Fig. 8 is the highest. Moreover, the average maximum link utilization with hysteresis is worse than that without hysteresis. These results show that the network performance does not strongly depend on the hysteresis threshold H itself. The VNT control method with demand hysteresis ($\alpha = 0.3$), the results of which are shown in Fig. 13, does not lead to a stable state. Since demand hysteresis is not effective compared with utilization hysteresis, in the next section, we will focus on utilization hysteresis and extend it to avoid slipping into undesirable stable states.

4. Improvements in Network Performance

Applying utilization hysteresis to VNT control can improve the stability of the network, but cannot always improve the performance, as discussed in the previous section. In this section, we extend utilization hysteresis to improve both the stability and performance.

4.A. Two-State Utilization Hysteresis

As we discussed in Section 3, utilization hysteresis can improve the network stability, but cannot always converge to a state that has lower maximum link utilization. Route flapping occurs, and the routes of the overlay network oscillate between approximately two routes, which results in

high link utilization and relatively low link utilization if the VNT is fixed. Hence, the method with utilization hysteresis causes the VNT control to slip into a stable state when the hysteresis decides to continue using the current VNT for two consecutive rounds of VNT control. Therefore, we extended utilization hysteresis, called "*two-state utilization hysteresis*", to prevent VNT control from slipping into a stable state when the maximum link utilization is high. To do this, we introduced another threshold θ that determines whether utilization hysteresis is applied or not. If the current maximum link utilization u is higher than θ, utilization hysteresis is not applied to VNT control so that it does not slip into an undesirable state, where u is high. Otherwise, utilization hysteresis, described in Section 3, is performed. We define the threshold $\theta = u_l + (u_u - u_l)/k$, where u_l and u_u are the minimum and maximum value of the maximum link utilization obtained up to this point, respectively, and k is a control parameter for adjusting θ. The utilizations u_l and u_u are updated every time VNT control is performed. When u is higher than θ, VNT control regards the maximum link utilization of the current VNT as high. In this case, utilization hysteresis is not applied to VNT control, and the VNT is immediately reconfigured so that it does not slip into a stable state that has high maximum link utilization. Then VNT control again searches for another stable state where the maximum link utilization is sufficiently low.

4.B. Performance Evaluation

We evaluated two-state utilization hysteresis under the same simulation model as the one described in the previous section. The simulation parameters were set to the same as those in Fig. 12. Figures 14 and 15 respectively show the fluctuation of the maximum link utilization in the case that k is 3.0 and 5.0. These figures clearly show that VNT control becomes stable and the maximum link utilization is lower than that shown in Figure 12. However, these figures also show that the convergence time, which is defined as the period of time before the VNT is stable, becomes longer than that shown in Fig. 12. This is because a larger value of k places more restriction on the region where utilization hysteresis is applied and thus seeking a stable state that has lower maximum link utilization is difficult. In the next section, we show another extension that shortens the convergence time.

5. Fast Convergence of VNT Control

In this section, we introduce a *filtering* method to achieve fast convergence of VNT control with two-state utilization hysteresis.

5.A. Filtering Method to Achieve Fast Convergence

As mentioned in the previous section, the convergence time is longer if the VNT control method with two-state utilization hysteresis is used. Since two-state utilization hysteresis restricts the region in which utilization hysteresis is applied, the chances that VNT control converges to a stable state decrease and therefore the convergence time becomes longer. When utilization hysteresis is not applied due to the high maximum link utilization, the VNT is reconfigured in the same way as the VNT control method without utilization hysteresis. These changes in the VNTs lead to network

instability. To achieve fast convergence, a mechanism to reduce the changes in VNTs is needed.

To investigate changes in VNTs in more detail, we observed the number of lightpaths between node pairs. We selected two node pairs that have a typical tendency, and we show the results of using these node pairs in Fig. 16. The horizontal axis shows the rounds, and the vertical axis shows the number of lightpaths between a node pair. In Fig. 16(a), one lightpath is configured from node 0 to 1 at most rounds, and the number of lightpaths finally converges to 1; however, only at rounds 60, 160, and 350, are two lightpaths configured. In Fig. 16(b), two lightpaths are configured at almost all the rounds, and the number of lightpaths finally converges to 2, although the number of lightpaths decreases or increases in a short period. We find these results in more than half of all the node pairs. We refer to these small changes in the number of lightpaths as "spike lightpath changes". These multiple spike lightpath changes lead to a large change in VNT and the network instability.

To achieve fast convergence of VNT control, we introduced a filtering method to VNT control that reduces the spike lightpath changes. The VNT control method with filtering remembers the number of lightpaths that the VNT control method has calculated, that is, $C^h(t) = \{c_p^h(t)\}$, described in Section 3. Here, the history of the past T rounds of the VNT control method is maintained, $(C^h(t-2), C^h(t-4), \ldots, C^h(t-2T))$. If n lightpaths were configured between a node pair p at more than $x\%$ of rounds in this history, the number of lightpaths between p is set to n, even if $c_p^h(t)$ is different from n. This is how the filtering method reduces the spike lightpath changes and thus achieves fast convergence. In the following subsection, we show that the filtering method reduces the convergence time of VNT control.

5.B. Performance Evaluation

We evaluated the filtering method under the same simulation environments as those described in the previous section. The simulation parameters were set to the same as those in Fig. 15. The convergence time in Fig. 17(b) is 72% shorter than that in Fig. 15(a). In the case that $H = 0.4$, the convergence time with the filtering method is also 71% rounds shorter than that without the filtering method. The maximum link utilization in the stable state is almost the same since the filtering method only reduces the spike lightpath changes, and the generated VNT is almost the same as the VNT generated by VNT control without the filtering method. These results show that the filtering method enhances the feasibility of the real network by reducing the convergence time.

We next evaluated adaptability for changes in the traffic demand in the situation when the traffic demand is dynamically changed. To evaluate the adaptability, we randomly generated the traffic demand at the same interval of rounds while keeping the sum of the traffic demand constant. We refer to this interval as the "changing interval". The other simulation conditions we used are the same as those described in the previous section. Figure 18 shows that the maximum link utilization depends on the rounds for $k = 3.0$. In the case that the changing interval is 40 (i.e., 20 VNT reconfigurations), VNT control follows almost all the changes in the traffic demand. However, only at rounds 1440 and 1480 does the VNT control not converge until the next traffic change occurs. If the changing interval is longer than 40, VNT control converges, although the maximum link

utilization fluctuates for a short period after the traffic change occurs. We next evaluated the adaptability for $k = 5.0$. The results of our evaluation are shown in Fig. 19. VNT control cannot follow the changes in the traffic demand in the case that the changing interval is 40. As we mentioned in Section 4, the region where hysteresis is applied becomes narrow and therefore the convergence time becomes longer if the large k is used. This also leads to the degradation of the adaptability for the traffic changes. In the case that the changing interval is 100, VNT control follows almost all the changes in the traffic demand except at round 200. Although our methods do not always follow extremely heavy changes in the traffic demand, they follow almost all the changes. The reason for this is that VNT control with the hysteresis mechanism reconfigures its VNT immediately to adapt to changes in the traffic demand if the performance of the VNT is degraded due to changes in the traffic demand.

6. Conclusion

In this paper, we discussed the selfish behavior of overlay routing on top of a VNT. We revealed that the dynamics of overlay routing cause high fluctuations in traffic demand, which lead to a significant VNT control instability. To overcome the traffic demand fluctuation and to make VNT control more stable, we applied demand hysteresis and utilization hysteresis to VNT control. We found that demand hysteresis improves the stability in terms of the number of changed lightpaths, but does not provide the stable maximum link utilization, especially when the overlay traffic ratio is large. We also found that utilization hysteresis improves the stability, but cannot always improve the maximum link utilization. Because of this, we proposed a two-state utilization hysteresis method that applies utilization hysteresis only when the maximum link utilization is sufficiently low. Simulation results show that two-state utilization hysteresis improves both the stability and the maximum link utilization. However, the convergence time becomes longer. To achieve faster convergence, we introduced a filtering method to the VNT control method with two-state utilization hysteresis. Through simulations, we showed that the filtering method reduces the convergence time. Both the hysteresis method and filtering method aim at improving the VNT control stability by reducing unnecessary changes in the VNT. In general, these types of approaches degrade the adaptability for changes in the traffic demand since the two methods tend to continue using the VNT designed for the old traffic demand. Although the VNT control method with two-state utilization hysteresis and filtering do not always follow extremely heavy changes in the traffic demand, it follows almost all the changes.

References

1. J. Li, G. Mohan, E. C. Tien, and K. C. Chua, "Dynamic routing with inaccurate link state information in integrated IP over WDM networks," Computer Networks **46**, 829–851 (2004).
2. T. Ye, Q. Zeng, Y. Su, L. Leng, W. Wei, Z. Zhang, W. Guo, and Y. Jin, "On-line integrated routing in dynamic multifiber IP/WDM networks," IEEE Journal on Selected Areas in Communications **22**, 1681–1691 (2004).

3. S. Arakawa, M. Murata, and H. Miyahara, "Functional partitioning for multi-layer survivability in IP over WDM networks," IEICE Transactions on Communications **E83-B**, 2224–2233 (2000).
4. N. Ghani, S. Dixit, and T.-S. Wang, "On IP-over-WDM integration," IEEE Communications Magazine **38**, 72–84 (2000).
5. M. Kodialam and T. V. Lakshman, "Integrated dynamic IP and wavelength routing in IP over WDM networks," in "Proceedings of IEEE INFOCOM," (2001), pp. 358–366.
6. J. Comellas, R. Martinez, J. Prat, V. Sales, and G. Junyent, "Integrated IP/WDM routing in GMPLS-based optical networks," IEEE Network Magazine **17**, 22–27 (2003).
7. Y. Koizumi, S. Arakawa, and M. Murata, "On the integration of IP routing and wavelength routing in IP over WDM networks," Proceedings of SPIE **6022**, 602205 (2005).
8. B. Mukherjee, D. Banerjee, S. Ramamurthy, and A. Mukherjee, "Some principles for designing a wide-area WDM optical network," IEEE/ACM Transactions on Networking **4**, 684–696 (1996).
9. R. Ramaswami and K. N. Sivarajan, "Design of logical topologies for wavelength-routed optical networks," IEEE Journal on Selected Areas in Communications **14**, 840–851 (1996).
10. D. G. Andersen, H. Balakrishnan, M. F. Kaashoek, and R. Morris, "Resilient overlay networks," in "Proceedings of SOSP," (2001), pp. 131–145.
11. S. Savage, T. Anderson, A. Aggarwal, D. Becker, N. Cardwell, A. Collins, E. Hoffman, J. Snell, A. Vahdat, G. Voelker, and J. Zahorjan, "Detour: a case for informed internet routing and transport," IEEE Micro **19**, 50–59 (1999).
12. Y. Liu, H. Zhang, W. Gong, and D. Towsley, "On the interaction between overlay routing and underlay routing," in "Proceedings of IEEE INFOCOM," (2005), pp. 2543–2553.
13. T. Roughgarden and E. Tardos, "How bad is selfish routing?" Journal of the ACM **49**, 236–259 (2002).
14. L. Qiu, Y. R. Yang, Y. Zhang, and S. Shenker, "On selfish routing in internet-like environments," in "Proceedings of ACM SIGCOMM," (2003), pp. 151–162.
15. W. Jiang, D.-M. Chiu, and J. C. S. Lui, "On the interaction of multiple overlay routing," Performance Evaluation **62**, 229–246 (2005).
16. M. Seshadri and R. H. Katz, "Dynamics of simultaneous overlay network routing," Tech. Rep. UCB/CSD-03-1291, EECS Department, University of California, Berkeley (2003).
17. C. S. R. Murthy and M. Gurusamy, *WDM Optical Networks Concepts, Design, and Algorithms* (Prentice Hall PTR Upper Saddle River, New Jersey 07458, 2002). ISBN 0-13-060637-5.
18. B. Mukherjee, *Optical WDM Networks* (Springer Verlag, New York, 2006). ISBN: 978-0-387-29055-3.
19. R. Dutta and G. N. Rouskas, "A survey of virtual topology design algorithms for wavelength routed optical networks," Optical Networks Magazine **1**, 73–89 (2000).
20. Y. Fukushima, S. Arakawa, M. Murata, and H. Miyahara, "Design of logical topology with effective waveband usage in IP over WDM networks," Photonic Network Communications **11**, 151–161 (2006).

21. J. Katou, S. Arakawa, and M. Murata, "A design method for logical topologies with stable packet routing in IP over WDM networks," IEICE Transactions on Communications **E86-B**, 2350–2357 (2003).
22. E. Leonardi, M. Mellia, and M. A. Marsan, "Algorithms for the logical topology design in WDM all-optical networks," Optical Networks Magazine **1**, 35–46 (2000).
23. R. Gao, C. Dovrolis, and E. W. Zegura, "Avoiding oscillations due to intelligent route control systems," in "Proceedings of IEEE INFOCOM," (2006), pp. 1–12.

List of Figures

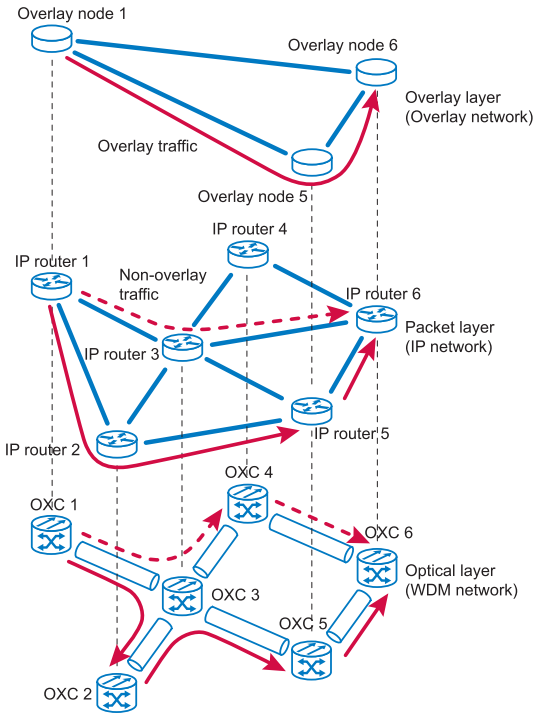

Fig. 1. Example of network consisting of three layers: optical, packet, and overlay

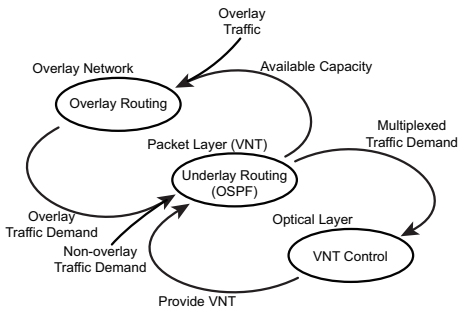

Fig. 2. Interaction between VNT control and overlay routing

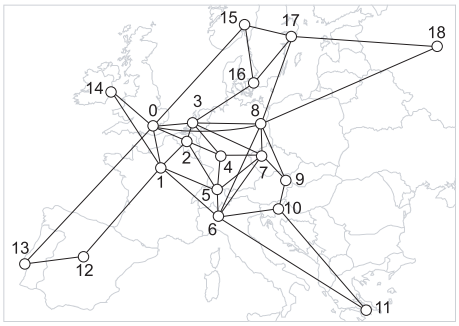

Fig. 3. European Optical Network topology

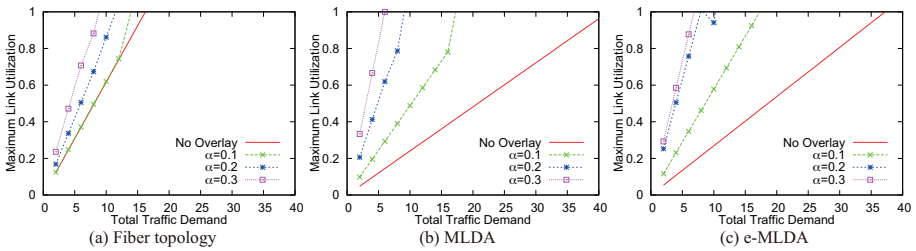

Fig. 4. Maximum link utilization

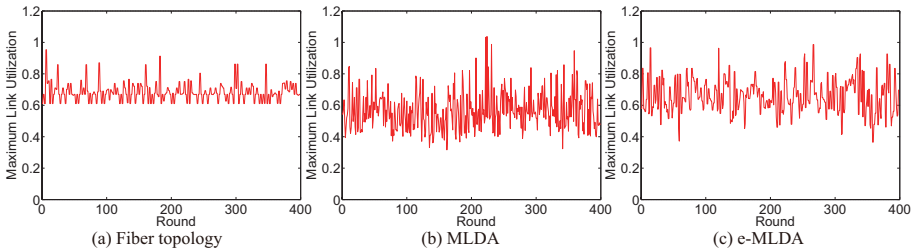

Fig. 5. Fluctuation of maximum link utilization ($\alpha = 0.2$, total traffic: 10)

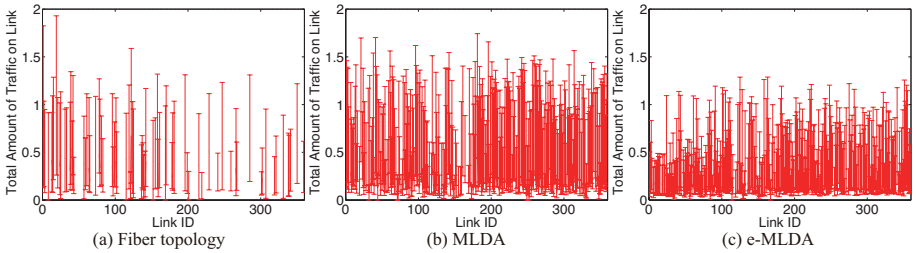

Fig. 6. Traffic volume on each link ($\alpha = 0.2$, total traffic: 10)

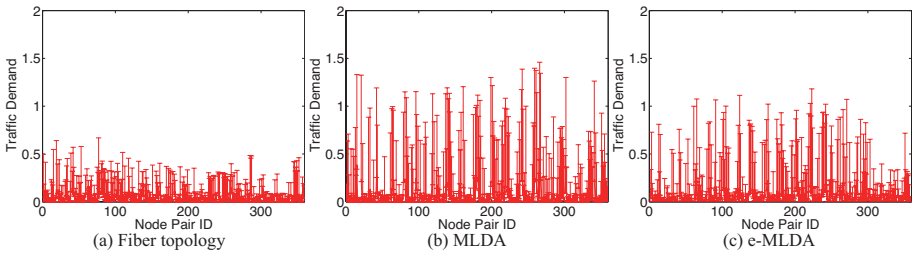

Fig. 7. Fluctuation of traffic demand ($\alpha = 0.2$, total traffic: 10)

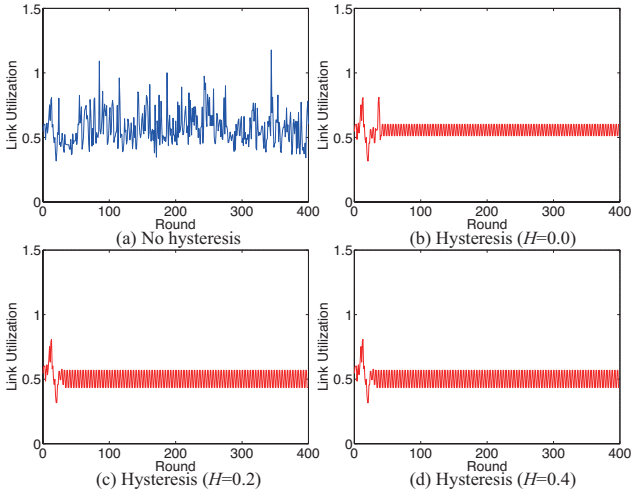

Fig. 8. Fluctuation of maximum link utilization (Utilization hysteresis, $\alpha = 0.2$, total traffic: 10)

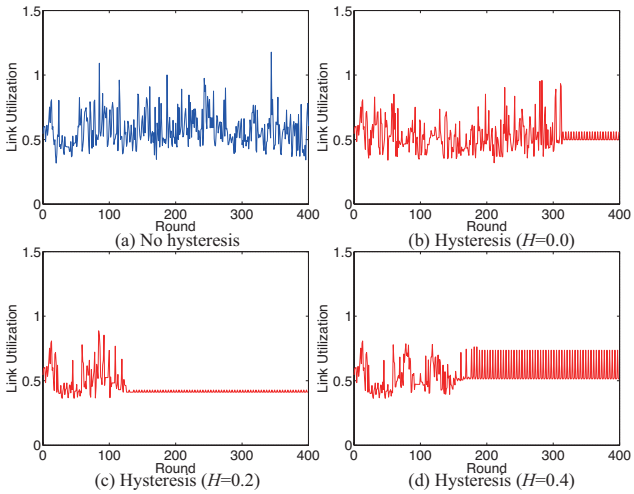

Fig. 9. Fluctuation of maximum link utilization (Demand hysteresis, $\alpha = 0.2$, total traffic: 10)

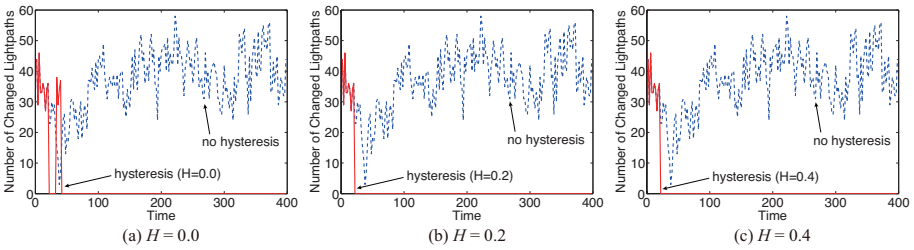

Fig. 10. Number of changed lightpaths (Utilization hysteresis, $\alpha = 0.2$, total traffic: 10)

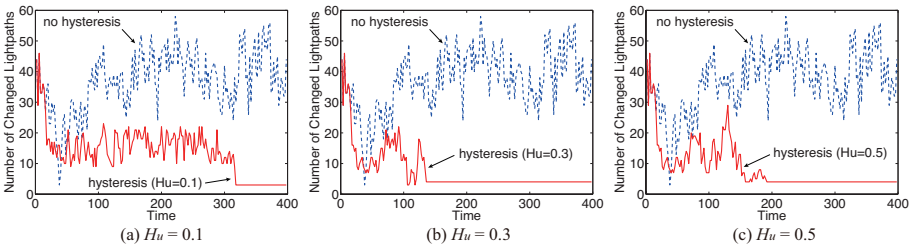

Fig. 11. Number of changed lightpaths (Demand hysteresis, $\alpha = 0.2$, total traffic: 10)

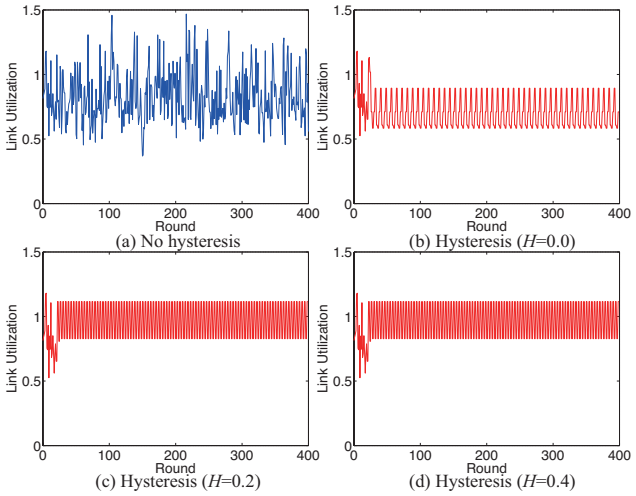

Fig. 12. Fluctuation of maximum link utilization (Utilization hysteresis, $\alpha = 0.3$, total traffic: 10)

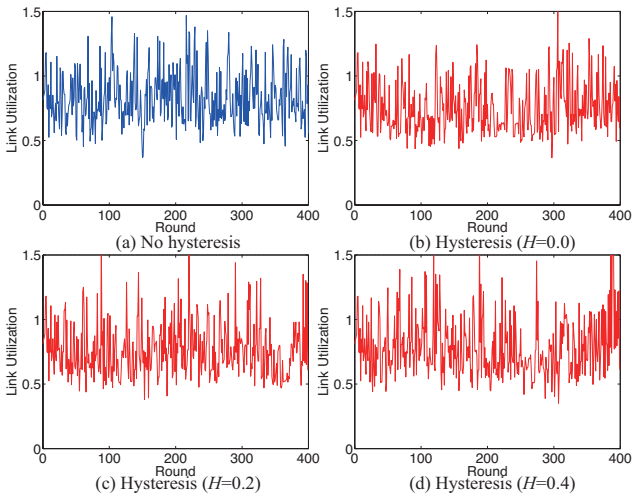

Fig. 13. Fluctuation of maximum link utilization (Demand hysteresis, $\alpha = 0.3$, total traffic: 10)

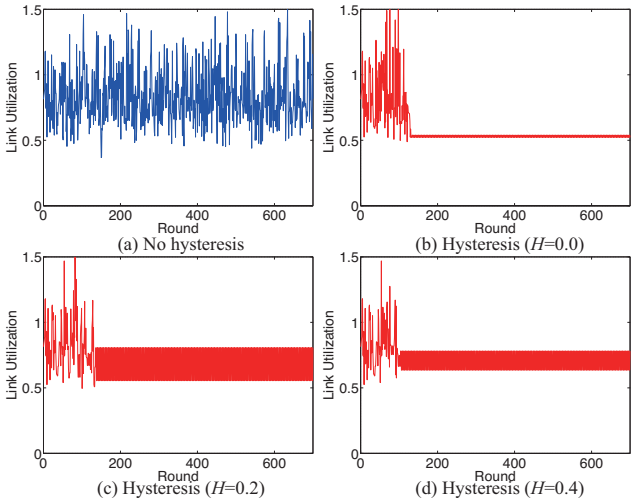

Fig. 14. Fluctuation of maximum link utilization (Two-state utilization hysteresis, $\alpha = 0.3$, total traffic: 10, $k = 3.0$)

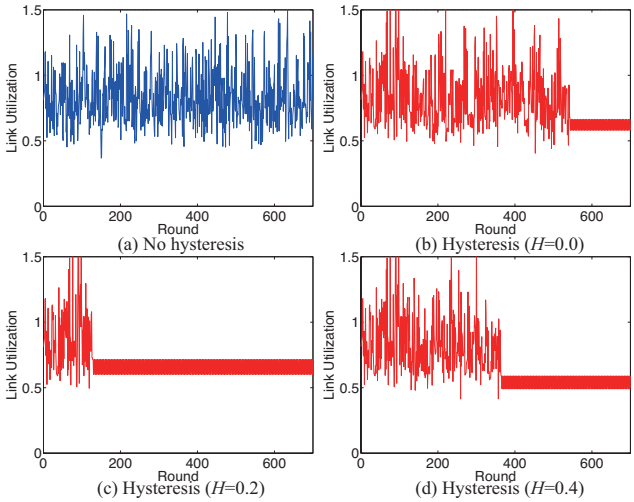

Fig. 15. Fluctuation of maximum link utilization (Two-state utilization hysteresis, $\alpha = 0.3$, total traffic: 10, $k = 5.0$)

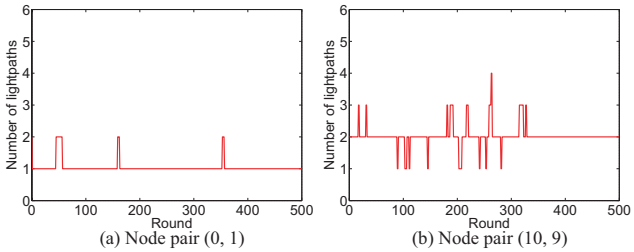

Fig. 16. Number of lightpaths ($\alpha = 0.3$, total traffic: 10, $k = 5.0$). Node ID in this figure is shown in Fig. 3.

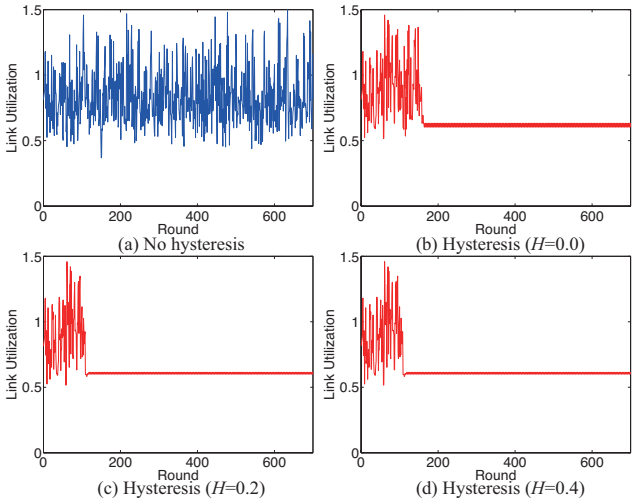

Fig. 17. Fluctuation of maximum link utilization (Two-state utilization hysteresis, filtering, $\alpha = 0.3$, total traffic: 10, $k = 5.0$)

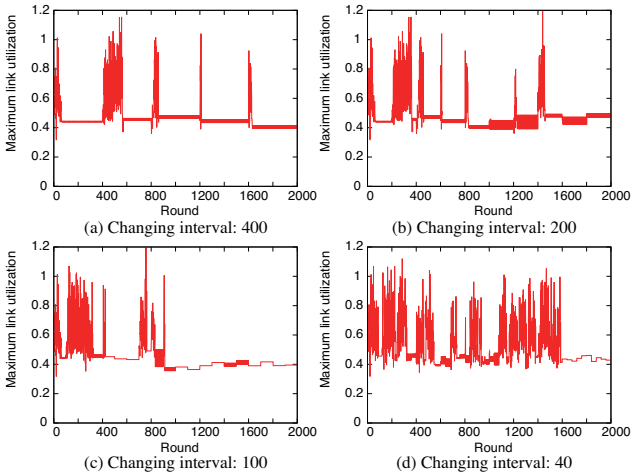

Fig. 18. Fluctuation of maximum link utilization (Two-state utilization hysteresis, filtering, $\alpha = 0.2$, total traffic: 10, $k = 3.0$)

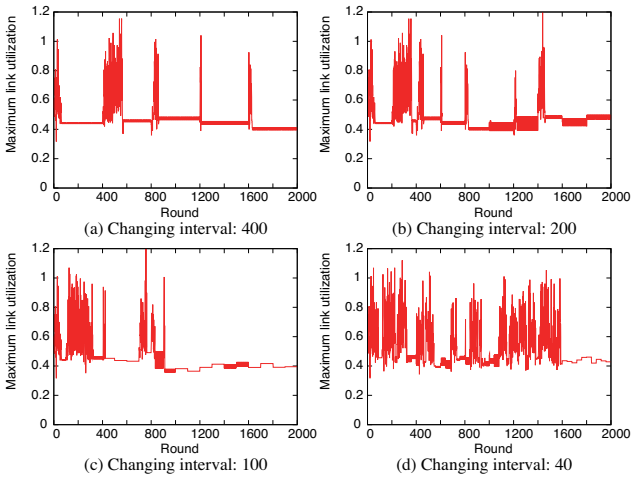

Fig. 19. Fluctuation of maximum link utilization (Two-state utilization hysteresis, filtering, $\alpha = 0.2$, total traffic: 10, $k = 5.0$)